Influence of the Submerged Arc Welding in the Mechanical Behaviour of the P355NL1 Steel. Part II: Analysis of the Low/High Cycle Fatigue Behaviours

Abílio M.P. De Jesus
University of Trás-os-Montes and Alto Douro, Engineering Department, Quinta de Prados, 5000-911 Vila Real, Portugal
ajesus@utad.pt

Alfredo S. Ribeiro
University of Trás-os-Montes and Alto Douro, Engineering Department, Quinta de Prados, 5000-911 Vila Real, Portugal

António A. Fernandes
University of Porto – Faculty of Engineering, Rua Dr. Roberto Frias, 4200-465 Porto, Portugal

Abstract. *A normalised fine grain carbon low alloy steel, P355NL1 (EN10028-3), intended for service in welded pressure vessels, where notch toughness is of high importance, has been investigated. Applications with this steel usually require the intensive use of welds. One of the most common welding processes that are used in the manufacturing of pressure vessels is the submerged arc welding. This welding process is often automated in order to perform the main seam welds of the body of the vessels. The influence of the automated submerged arc welding, in the mechanical performance, is investigated. In this paper, the low and high cycle fatigue and crack propagation behaviours are compared between base and welded materials. Several series of small and smooth specimens as well as cracked specimens made of base and welded materials, respectively, were fatigue tested. Strain, stress and energy based relations for fatigue life assessment are evaluated and compared between the base and welded materials. Finally, the fatigue crack propagation behaviours are compared between the base, welded and heat affected materials.*

Keywords*: P355NL1 steel, submerged arc welding, low cycle fatigue, high cycle fatigue, crack propagation*

1. Introduction

Pressure vessels are an important type of structures that usually experience, during operation, cyclic loads that lead to fatigue failures (Taylor *et al*, 2001). The design of this equipment should take into account all foreseeable degradation mechanisms, including fatigue. The need of including a fatigue assessment route in design of pressure equipment has been enforced by some important organizations (EC, 2001). It is a common industrial practice to use specific design codes such as the ASME VIII – Div. 2 (ASME, 2001), the PD5500 (BSI, 2003) and the recently approved EN 13445 (CEN, 2002). Alternative, more general and flexible procedures exist such as the local approaches (Radaj and Sonsino (1998) and Tricoteaux *et al* (1995)) or the Fracture Mechanics (De Jesus (2004) and Dijkstra *et al* (1987, 1993)) that can be used to model fatigue for both welded and unwelded structural details. The authors have developed important experimental investigations on the P355NL1 steel (De Jesus *et al*, 2005a). This material is well suited for pressure vessels industry, where high toughness and weldability are essential characteristics.

In this paper authors make a comparison of the mechanical behaviour between the P355NL1 steel − base material (BM) − and the welded material (WM), resulting from the submerged arc welding process, which is a very important welding process in the manufacturing of pressure vessels. The low and high cycle fatigue behaviours (fatigue resistances) are evaluated and compared between the BM and the WM. Strain-life, stress-life and energy-life experimentally based relations are proposed for those materials. Additionally, crack growth rates are determined for the BM, WM and for the material affected by the heat introduced by the welding process (HAZ). Results presented in this paper will be a valuable contribution for engineers concerned with fatigue assessment of pressure vessels using methodologies such as local approaches and Fracture Mechanics, applied separately or in conjunction.

2. Local approaches to fatigue

The local approaches constitute a very important methodology for the assessment of the fatigue behaviour of structural components. They are usually applied to model the initiation of fatigue cracks. They are based on the hypothesis that the behaviour of the material, in a critical location of a structural component, can be described using data from smooth specimens. The data obtained from tests of smooth specimens can be presented in several forms. The most common data is the strain-life data. Alternative data can also be proposed such as stress-life and energy-life data. Some relations for these three alternative forms are described in the next subsections.

2.1 Strain-life relations

Strain-life relations are mainly proposed to describe low cycle fatigue results. Typical relations have been suggested to correlate the strain amplitude with the number of reversals to failure, $2N_f$, usually considered to correspond to the initiation of a macroscopic crack (crack depth of 0.25 mm). The most used relation to model low cycle fatigue was proposed by Coffin (1954) and Manson (1953), which relates the plastic strain amplitude, $\Delta\varepsilon^p/2$, with the number of reversals to crack initiation, $2N_f$:

$$\frac{\Delta\varepsilon^p}{2} = \varepsilon'_f \left(2N_f\right)^c \tag{1}$$

where ε'_f and c are, respectively, the fatigue ductility coefficient and exponent. The Coffin-Manson relation can be extended to high cycle fatigue domains using the relation proposed by Basquin (1910). This relation relates the elastic strain amplitude, $\Delta\varepsilon^e/2$, with the number of reversals to failure:

$$\frac{\Delta\varepsilon^e}{2} = \frac{\Delta\sigma}{2E} = \frac{\sigma'_f}{E}\left(2N_f\right)^b \tag{2}$$

where σ'_f is the fatigue strength coefficient, b is the fatigue strength exponent and E is the Young modulus. The number of reversals corresponding to the transition between low and high cycle fatigue regimes is characterized by total strain amplitude, $\Delta\varepsilon/2$, composed by equal amplitudes of elastic and plastic strains. Lives below this transition value are dictated by ductility properties; lives above this transition value are dictated by strength properties. Morrow (1965) suggested the superposition of Eqs. (1) and (2), resulting a more general equation, valid for low and high cycle fatigue:

$$\frac{\Delta\varepsilon}{2} = \frac{\Delta\varepsilon^e}{2} + \frac{\Delta\varepsilon^p}{2} = \frac{\sigma'_f}{E}\left(2N_f\right)^b + \varepsilon'_f\left(2N_f\right)^c \tag{3}$$

2.2 Stress-life relations

Stress-life relations are used to correlate fatigue data obtained with fatigue tests of smooth specimens tested under stress control. Stress-life relations have been proposed mainly to assess high cycle fatigue. The Basquin relation (2) can be used in the form of a stress-life relation to model high cycle fatigue. Although being not consensual, some authors have proposed more sophisticated stress-life relations in order to model both low and high cycle fatigue regimes. An example of this type of relations was proposed by Lemaitre and Chaboche (1990):

$$N_f = \frac{\sigma_{UTS} - \sigma_{max}}{\sigma_{max} - \sigma_l\left(\sigma_{med}\right)}\left(\frac{\sigma_{max} - \sigma_{med}}{B_0\left(1 - \beta\sigma_{med}\right)}\right)^{\eta} \tag{4}$$

where σ_{max} and σ_{med} are, respectively, the maximum and mean controlled stresses of the cycle, $\sigma_l(\sigma_{med})$ is the endurance fatigue limit for a non null mean stress, σ_{UTS} is the ultimate tensile strength. The endurance fatigue limit, $\sigma_l(\sigma_{med})$, can be determined using a modified form of Goodman's equation (Lemaitre and Chaboche, 1990):

$$\sigma_l\left(\sigma_{med}\right) = \sigma_{med} + \sigma_{l0}\left(1 - \beta\sigma_{med}\right) \tag{5}$$

where σ_{l0} is the endurance fatigue limit for a fully-reversed loading and β is the slope of the assumed linear relation between the endurance fatigue limit and the mean stress. The endurance fatigue limits are expressed in the form of the maximum stress of the cycle. Constants β_0 and η are determined by fitting Eq. (4) to the experimental results of fully-reversed tests. Relation (4) was proposed to describe the complete Woehler curves, from the static rupture to the domain of fatigue endurance limits. It also describes the effect of the mean stress on the complete Woehler curves, including the mean stress effect on the fatigue endurance limit.

2.3 Energy-life relations

Stress-life and strain-life relations can be considered as classical or traditional local approaches. Modern local approaches have been proposed based on energy considerations, leading to the so called energy-life relations. The energy-life relations have been intensively investigated by several authors such as Halford (1966), Lefebvre and Ellyin (1984), Ellyin and Kujawski (1984), Golos and Ellyin (1988) and Ellyin (1997). The energy-life relations can be formulated with the following general form (Ellyin, 1997):

$$\psi = k(2N_f)^{\alpha} + \psi_0 \tag{6}$$

where ψ is an energy-based damage parameter, ψ_0 is an energy-based endurance fatigue limit, k ($k>0$) and α ($\alpha<0$) are constants resulting from a best fit technique of relation (6) to the experimental results.

Three common forms of energy-based damage parameters are the plastic strain energy density, the total strain energy density and a modified total strain energy density that takes into account the effect of the mean stress. The plastic strain energy density, per cycle, corresponds to the area of the hysteresis loops which, for a non-Masing material, has the following form (Lefebvre and Ellyin (1984), Ellyin and Kujawski (1984)):

$$\Delta W^p = \frac{1-n^*}{1+n^*}\Delta\sigma\Delta\varepsilon^p + \frac{2n^*}{1+n^*}\delta\sigma_0\Delta\varepsilon^p \tag{7}$$

where $\delta\sigma_0$ is the increase in the proportional stress limit that can be calculated using Eqs. (1) to (3) from reference (De Jesus *et al*, 2005b). The total strain energy density, per cycle, is given by the following formula:

$$\Delta W = \frac{1}{2}\Delta W^p + \frac{1}{2}\Delta\sigma\Delta\varepsilon \tag{8}$$

The parameters ΔW and ΔW^p are suitable only for fully- or almost fully-reversed tests, because they are not sensitive to the mean stress. Golos and Ellyin (1988) proposed another version of the total strain energy density, ΔW^t. This energy is equal to the plastic strain energy density, defined in Eq. (7), plus the elastic strain energy density associated to the tensile stress of the cycle, ΔW^{e+}, defined as follows:

$$\Delta W^{e+} = \frac{1}{2E}\left(\frac{\Delta\sigma}{2}+\sigma_{med}\right)^2 = \frac{\sigma_{max}^2}{2E} \tag{9}$$

3. Fracture Mechanics approach

The Fracture Mechanics approach can be used as an alternative to the local approaches (Dijkstra *et al*, 1987, 1993). This approach is based on the pre-existence of a small defect or flaw which is assumed to be an initial crack. Fracture Mechanics models the propagation of fatigue cracks from an initial size to final dimensions responsible for the fracture of structural components. Fracture Mechanics can also be used to complement the local approaches (Ribeiro, 1993). Local approaches are used to model the initiation of a macroscopic crack and Fracture Mechanics approaches are used to model the propagation of the initial macroscopic crack until rupture occurs. Thus, the total number of cycles to ultimate failure, N_f, can be expressed as follows:

$$N_f = N_i + N_P \tag{10}$$

where N_i is the number of cycles required to initiate a crack and N_P is the number of cycles required to propagate the crack.

The Linear Elastic Fracture Mechanics (LEFM) is a well established branch of Fracture Mechanics that has been applied intensively to the propagation period of fatigue cracks (Sanford, 1997). The LEFM is based on the hypothesis that the stress intensity factor, K, is the mechanical parameter that controls the stress range at the crack tip. Several laws have been proposed to characterize the fatigue crack propagation rates, combining the da/dN and ΔK parameters. A well known classical relation was proposed by Paris *et al* (1961, 1963) and has the following form:

$$\frac{da}{dN} = C\left(\Delta K\right)^m \tag{11}$$

where da/dN is the fatigue crack propagation rate, $\Delta K = K_{max}-K_{min}$ represents the range of the stress intensity factor and C and m are material constants. Many other relations have been proposed (Hoeppner e Krupp, 1974), but due to its simplicity and reasonable domain of applicability, the Paris relation is widely applied. Walker (1970) proposed a modification to the Paris's law in order to take into account the mean stress effect:

$$\frac{da}{dN} = C\left[\Delta K/\left(1-R_\sigma\right)^{1-\lambda}\right]^m \tag{12}$$

where C and m are the constants of the Paris's law for R_σ=-1; λ is a constant that allows the correlation of crack propagation data for several stress ratios.

4. Materials characterization and experimental details

This paper presents experimental fatigue data obtained for the carbon low alloy steel P355NL1, delivered in the form of plates with 5.1 mm thickness. This designation is according to the EN10028-3 standard (CEN, 2003). This steel has the former designation of TStE355, specified in the DIN 17102 standard (DIN, 1983). This steel is a weldable normalized fine grain structural steel, applied for pressure vessel purposes with special requirements for low temperatures. Materials resulting from the automated submerged arc welding are also investigated, namely the welded material and the material affected by the heat introduced by the welding process. The fatigue behaviours of these materials are compared based on an experimental program. Details about the investigated materials are addressed by De Jesus *et al* (2005b).

Fatigue tests were performed on smooth and small specimens manufactured according to the ASTM E606 standard (ASTM, 1998). A total of nine series of specimens were tested, four under strain control ($2\times R_\varepsilon=-1$, $2\times R_\varepsilon=0$) and five under stress control ($2\times R_\sigma=-1$, $R_\sigma=-0.5$, $2\times R_\sigma=0$), resulting in a total of 127 tested specimens. Five series of specimens are made of base material (BM); four series have welded material at the gauge length. Details about the preparation of the specimens, descriptions of the series and fatigue tests can be found in De Jesus *et al* (2005b).

This paper also presents results from fatigue crack propagation tests conducted on cracked CT specimens. The geometry and test procedures were defined according to the ASTM E647 standard (ASTM, 1999). The specimens were prepared in order to present BM, WM and HAZ materials on the crack path. Thus, crack propagation behaviours will be assessed for the referred materials. The CT specimens have a width, L, equal to 50 mm and a height, H, equal to 48 mm. The thickness of the specimens was 4.35 mm. A total of 14 CT specimens were tested under pulsating stress covering three stress ratios ($R_\sigma=0$, $R_\sigma=0.5$ and $R_\sigma=0.7$) and three materials.

5. Results and discussion

5.1. Strain-life relations

Figure 1 presents the strain-life data obtained in this research. Figure 1a presents the total strain *versus* life data; Fig. 1b presents the plastic strain *versus* life data and Fig. 1c presents the elastic strain *versus* life data. The data was obtained for the base material – the P355NL1 steel – and also for the welded material. Two strain ratios were investigated. The analysis of the data shows that the two materials have similar fatigue strength behaviours as revealed by the elastic strain *versus* life data. The plastic strain *versus* life data shows distinct fatigue ductility behaviours of the base and welded materials. The effect of the strain ratio on the strain-life data is negligible for the base material. This is explained by the complete cyclic mean stress relaxation observed for tests conducted under null strain ratio. The welded material exhibits a strain-life behaviour which slightly depends on the strain ratio. This is due to the fact that, in general, the welded material exhibits higher resistance to cyclic mean stress relaxation than base material, in particular for tests conducted under null strain ratio.

Table 1 presents the constants for the strain-life relation (3). These constants were derived for $R_\varepsilon=-1$ and $R_\varepsilon=0$ and also for the conjunction of both data. Constants are proposed for the base and welded materials. The correlation coefficients are also included in the Tab.1. The number of cycles corresponding to the transition between the fatigue behaviour governed by ductility and the fatigue behaviour governed by strength properties are also included in Tab. 1. It can be observed that the base material presents a transition number of cycles about ten times higher than the welded material. For the welded material the strength properties are dominant for a wider fatigue range than that observed for the base material.

Table 1. Constants for the strain-life relations of the base and welded materials.

Constants	**Base Material**			**Welded Material**		
	$R_\varepsilon=-1$	$R_\varepsilon=0$	$R_\varepsilon=-1+R_\varepsilon=0$	$R_\varepsilon=-1$	$R_\varepsilon=0$	$R_\varepsilon=-1+R_\varepsilon=0$
σ'_f [MPa]	1087.6	923.4	1005.5	1128.6	1026.0	1067.0
b [-]	-0.1090	-0.0955	-0.1033	-0.1086	-0.0958	-0.1007
R^2	0.9641	0.8611	0.9140	0.9854	0.9839	0.9827
ε'_f [-]	0.4108	0.2933	0.3678	4.9545	1.0249	3.7473
c [-]	-0.5547	-0.5311	-0.5475	-1.0017	-0.8119	-0.9805
R^2	0.9918	0.9695	0.9795	0.9826	0.9540	0.9413
$2N_T$	17344	14500	16500	2042	1725	1807
$\Delta\varepsilon_T/2$ [%]	0.365	0.361	0.360	0.481	0.245	0.489

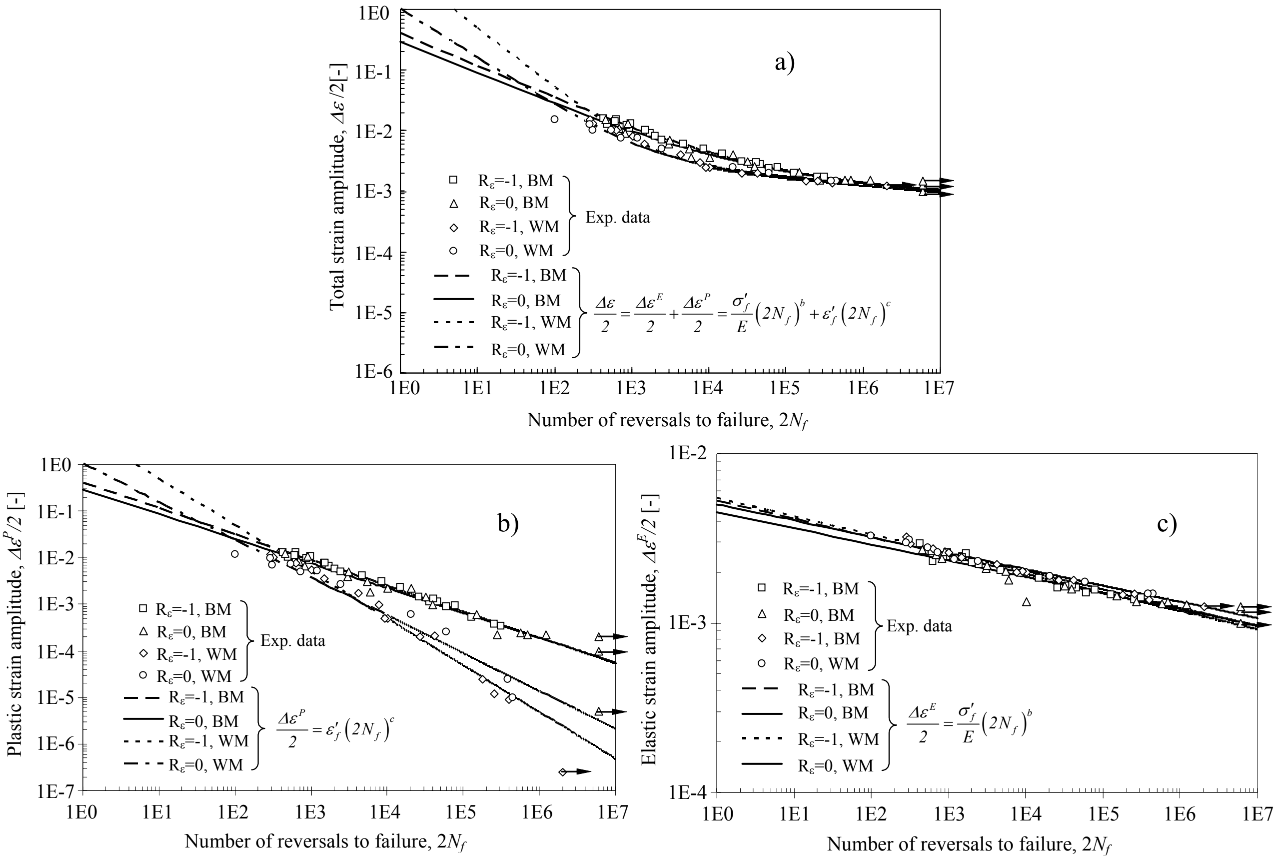

Figure 1. Strain–life data for BM and WM: a) total strain data; plastic strain data; elastic strain data.

5.2. Stress-life relations

This paper also reports fatigue tests of smooth specimens carried out under stress control. Three stress ratios were tested for the BM (R_σ=-1, R_σ=-0.5 and R_σ=0.0); two stress ratios were investigated for the WM (R_σ=-1 and R_σ=0.0). Figure 2 presents all experimental data. The same figure also includes the curves obtained by the best fit of Eq. (4) to the experimental data. Table 2 summarizes the constants resulting from the referred curve fitting. It can be concluded that the expression proposed by Lemaitre and Chaboche (1990) gives an overall good description. Although some difficulties are encountered in the description of the Woehler's curves, in particular for the low cycle fatigue domain with R_σ=0. The mean stress effect is reasonably captured by the model as well as the static rupture and the fatigue endurance asymptotes. Is more or less well established that low cycle fatigue domain is best described using strain-life relations rather than stress-life relations.

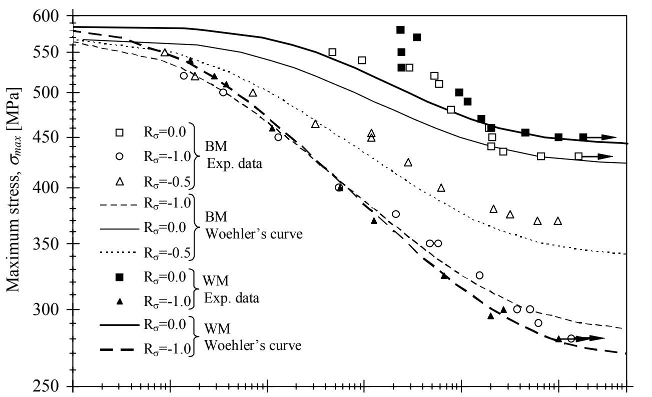

Figure 2. Stress-life data and Woehler's correlations.

Table 2 – Constants required for the description of the Woehler's curves according to Eq. (4).

Material	η	B_0 [MPa]	β [1/MPa]	$\sigma_{max,lf\,0}$ [MPa]	σ_u [MPa]
BM	6.2	1561.6	0.001209	284.2	568.11
WM	5.6	1785.7	0.000779	267.4	585

5.3. Energy-life relations

Figure 3 illustrates the energy-life relations obtained for the BM and WM, using the damage parameters described in equations (7) to (9). The endurance fatigue limits are defined as being the strain energy density leading to two million reversals of failure. The proposed energy-life relations were derived from the strain-life data obtained for $R_\varepsilon=-1$. The proposed energy-life relations are in close agreement with the experimental data. Table 3 summarizes the constants of the energy-life equation (6). In general, WM exhibits lower fatigue resistance than BM. This difference is much more pronounced if the plastic strain energy density is used as a damage parameter. The difference is minimal if the total strain energy is used as a damage parameter. The observed differences between the two materials are less important for low cycle fatigue regime than for high cycle fatigue.

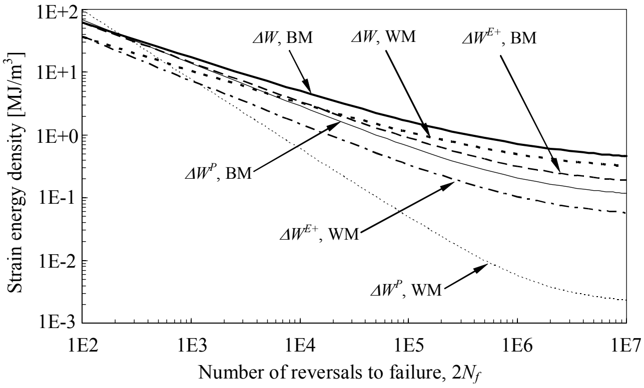

Figure 3. Energy-life relations.

Table 3. Constants for the energy-life relations for the BM and WM.

Material	k^P	α^P	ΔW_0^P	k	α	ΔW	k^t	α^t	ΔW_0^t
	MJ/m^3	-	MJ/m^3	MJ/m^3	-	MJ/m^3	MJ/m^3	-	MJ/m^3
BM	1671.5	-0.695	0.094	787.9	-0.557	0.361	1163.8	-0.640	0.149
WM	15544.7	-1.105	0.002	431.7	-0.542	0.249	918.2	-0.700	0.046

5.4 Crack propagation data

This paper also compares the crack propagation behaviour between the BM, the WM and the HAZ. Three stress ratios were investigated: $R_\sigma=0.0$, $R_\sigma=0.5$ and $R_\sigma=0.7$. The last stress ratio was only tested for the BM and WM. Figure 4 presents the experimental crack propagation curves. Table 4 summarizes the constants resulting from the best fit of the Paris and Walker equations to the experimental data. Results show that for null stress ratio (Fig. 4a) the BM has higher crack propagation rates than WM and HAZ. The BM and HAZ exhibits very similar crack propagation behaviours for all stress ratios considered. For a stress ratio equal to 0.5 (Fig. 4b) the three materials exhibit very similar behaviours. The increase of the stress ratio produces an increase on crack propagation rates as demonstrates Fig. 4d for the BM. The Walker relation was able of describing the effect of stress ratio.

The crack propagation tests generated crack growth data covering, essentially, the region II of propagation. In this region the crack propagation data shows a linear relationship as demonstrated by the results of Fig. 4. The influence of the stress ratio is less pronounced in region II, than in propagation regions I and III. In fact, the analysis of Fig. 4d shows a small influence of stress ratio on crack growth data. Similar behaviours were observed for the WM and HAZ. Also, it has been demonstrated that materials microstructure has small influence in region II fatigue crack growth (Maddox (1974) and James (1977)). This is not true for region I – the near threshold region. This conclusion is verified in this research since the overall scatter band for all data (materials and stress ratios) was narrow. It is interesting to note that James (1977) performed its investigations using pressure vessels weldments as was done in this work.

In this research no residual stress measurements were performed on CT specimens. Although, authors believe that eventual residual stresses introduced by the welds were minimized since the specimens are cut from a larger plate and their dimensions are relatively small. These conditions promote the relief of the residual stresses.

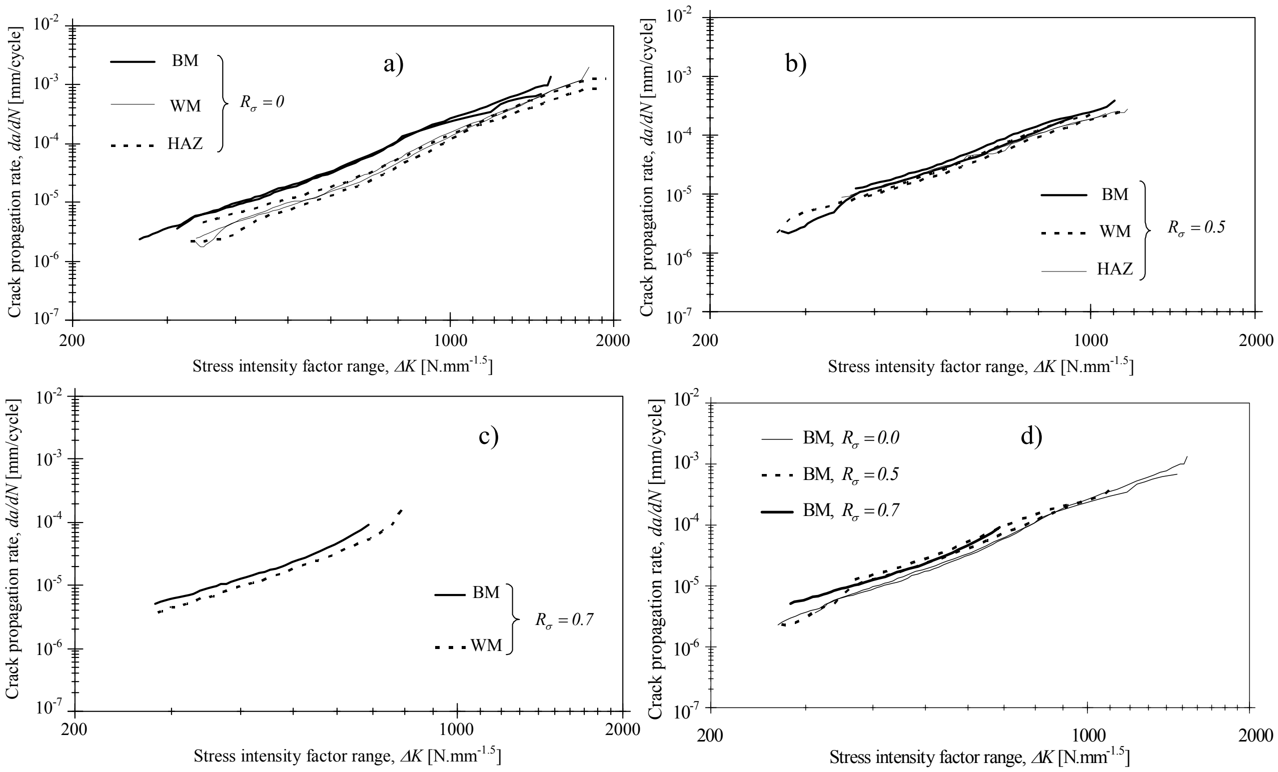

Figure 4. *da/dN* - *ΔK* curves for BM, WM and HAZ: a) $R_\sigma=0$; b) $R_\sigma=0.5$; c) $R_\sigma=0.7$; d) BM ($R_\sigma=0+ R_\sigma=0.5+ R_\sigma=0.7$).

Table 4. Crack propagation constants according to the Paris's law for BM, WM and HAZ.

	Base Material			**Welded Material**			**HAZ**	
R_σ	**0.0**	**0.5**	**0.7**	**0.0**	**0.5**	**0.7**	**0.0**	**0.5**
m	3.499	3.555	3.003	3.905	3.192	3.156	3.673	2.975
C	7.195E-15	6.281E-15	2.037E-13	2.615E-16	5.199E-14	6.104E-14	1.141E-15	2.258E-13
R^2	0.996	0.984	0.985	0.994	0.991	0.981	0.984	0.997
λ	0.92			0.78			0.67	

da/dN: mm/cycle; K: N.mm$^{-1.5}$

6. Conclusions

A comparison between the low and high cycle fatigue behaviours of a BM – the P355NL1 steel – and a WM resulting from the automated submerged arc welding was characterized based on stress- and strain-controlled fatigue tests of smooth specimens. A comparison of the crack propagation behaviours between the BM, WM and HAZ was also performed using results from fatigue tests of cracked specimens. The comparisons evidenced some distinct behaviours between the materials considered, which justifies a special attention by engineers concerned with the application of the local approaches plus LEFM to assess welded details. The following main conclusions can be stated:

- Strain-life data was obtained for BM and WM covering two strain ratios namely $R_\varepsilon=0$ and $R_\varepsilon=-1$. The strain ratio has negligible influence on strain-life behaviour for the two materials. The BM and WM present similar fatigue strength behaviours which justify same fatigue endurance limits. The fatigue ductility behaviours are clearly distinct between the BM and WM. However, this discrepancy only produces a relative small scatter on the global strain-life data. Extrapolations for very low cycle fatigue regions foresee important differences between the fatigue behaviour of the two materials. More experimental data is required in order to increase the confidence of the proposed data for this domain.
- Stress-life relations were proposed based on stress-controlled fatigue data. The representation of Woehler's curves proposed by Lemaitre and Chaboche fairly describes the data in all fatigue domains. The proposed relation encounters some difficulties for null stress ratio and higher maximum stresses. The full-reversed data indicates

similar behaviours for the BM and WM with the exception of the fatigue endurance domain. These conclusions can be extended for null-stress ratio data.

- Energy-life relations were derived from the strain-life data. These relations indicate that the fatigue resistance of the WM, defined in terms of the strain energy density of the cycle, is lower than observed for the BM.
- The BM presents slightly higher crack growth rates than WM and HAZ, for null stress ratio. For stress ratios equal to 0.5 and 0.7 the differences between crack growth rates are almost negligible. The influence of stress ratio is small. In general, crack growth rates obtained for all materials (three distinct microstructures) and stress ratios fall in a narrow band, which is in agreement with results published in literature for this type of materials and weldments.

7. References

ASME – The American Society of Mechanical Engineers, 2001, "ASME Boiler and Pressure Vessel Code – Section VIII: Rules for Construction of Pressure Vessels, Division 2 – Alternative rules, Appendix 5: Design based on fatigue analysis", New York.

ASTM, American Society for Testing and Materials, 1998, "ASTM E606-92: Standard Practice for Strain-Controlled Fatigue Testing", In Annual Book of ASTM Standards, ASTM, West Conshohocken, PA, Part 10, pp. 557-571.

ASTM, American Society for Testing and Materials, 1999, "ASTM E647: Standard Test Method for Measurement of Fatigue Crack Growth Rates", In Annual Book of ASTM Standards, Vol. 03.01, ASTM, West Conshohocken, PA, pp. 591-629.

Basquin, O. H., 1910, "The Exponential Law of Endurance Tests", Proceedings of ASTM, Vol. 10 (II), pp. 625-630.

BSI – British Standards Institution, 2003, "PD 5500:2003, Specifications for unfired fusion welded pressure vessels", British Standard, London.

CEN, European Committee for Standardization, 2002, "EN 13445:2002 - Unfired Pressure Vessels", European Standard.

CEN, European Committee for Standardization, 2003, "EN 10028-3. Flat Products Made of Steels for Pressure Purposes - Part 3: Weldable Fine Grain Steels, Normalized", European Standard.

Coffin, L.F., 1954, "A study of the Effects of Cyclic Thermal Stresses on a Ductile Metal", Translations of the ASME, Vol.76, No. 6, pp. 931-950.

De Jesus, A.M.P., 2004, "Validação de Procedimentos de Cálculo à Fadiga de Reservatórios sob Pressão", PhD Thesis, University of Trás-os-Montes e Alto Douro, Vila Real, Portugal.

De Jesus, A.M.P, Ribeiro, A.S., Fernandes, A.A., 2005a, "Low and High Cycle Fatigue and Cyclic Elasto-Plastic Behaviour of the P355NL1 Steel", Journal of Pressure Vessel Technology (submitted on December 2004, accepted for publication on June 2005).

De Jesus, A.M.P, Ribeiro, A.S., Fernandes, A.A., 2005b, "Influence of the Submerged Arc Welding in the Mechanical Behaviour of the P355NL1 steel. Part I: Analysis of the Cyclic Elastoplastic Behaviour", XVIII COBEM (conditionally accepted).

Dijkstra, O.D., Snijder, H.H., Overbeeke, J.L., Wildschut, 1987, "Prediction of fatigue crack growth for welded joints using stress intensity factors determined by FEM calculations", SIMS'87, Delft, The Netherlands.

Dijkstra, O.D., van Straalen, I.J.J., Noordhoek, C., 1993, "A fracture mechanics approach of fatigue of welded joints in offshore structures", OMAE'93 –International Conference on Offshore Mechanics and Arctic Engineering, Glasgow, Scotland.

DIN, Deutsche Institute for Standardization, 1983, "DIN 17102: Weldable Normalized Fine Grain Structural Steels. Technical Delivery Conditions for Plate, Strip, Wide Flats, Sections and Bars", Deutsche Norm.

EC, European Commission, 2001, "Pressure components fatigue design in the framework of directive 97/23/EC on pressure equipment. Final Report", DG-JRC/IAM, Petten – The Netherlands: http//www.ped.eurodyn.com/

Ellyin, F., 1997, "Fatigue Damage, Crack Growth and Life Prediction", Chapman & Hall, London, UK.

Ellyin, F., and Kujawski, D., 1984, "Plastic Strain Energy in Fatigue Failure", Journal of Pressure Vessel Technology, Translations of the ASME, Vol.106, No. 4, pp. 342-347.

Golos, K., and Ellyin, F., 1988, "A Total Strain Energy Density Theory for Cumulative Fatigue Damage", Journal of Pressure Vessel Technology, Translations of the ASME, Vol.110, pp. 36-41.

Halford, G. R., 1966, "The Energy Required for Fatigue", Journal of Materials, Vol.1, No. 1, pp. 3-18.

Hoeppner, D. W., Krupp, W. E., 1974, "Prediction of component life by application of fatigue crack growth knowledge", Engineering Fracture Mechanics, Vol.6, pp. 47-70.

James, L. A., 1977, "Fatigue-crack propagation behaviour of several pressure vessel steels and weldments", Welding Journal, Vol.56, p. 386.

Lefebvre, D., and Ellyin, F., 1984, "Cyclic Response and Inelastic Strain Energy in Low Cycle Fatigue", International Journal of Fatigue, Vol.6, No. 1, pp. 9-15.

Lemaitre, J., and Chaboche, J.L., 1990, "Mechanics of Solid Materials", Cambridge University Press, Cambridge, UK.

Maddox, S. J., 1974, "Assessing the significance of flaws in welds subjected to fatigue", Welding Journal, Vol.53, p. 401.

Manson, S.S., 1953, "Behaviour of Materials Under Conditions of Thermal Stress", Technical Report No.1170, National Advisory Committee for Aeronautics, NACA.

Morrow J. D., 1965, "Cyclic Plastic Strain Energy and Fatigue of Metals", In Internal Friction, Damping and Cyclic Plasticity, ASTM STP 378, American Society for Testing and Materials, Philadelphia, PA, pp. 45-87.

Paris, P.C., Gomez, M.P., Anderson, W.E., 1961, "A rational analytic theory of fatigue", The Trend in Engineering, Vol.13, No. 1, pp. 9-14.

Paris, P.C., Erdogan, F., 1963, "A critical analysis of crack propagation laws", Journal of Basic Engineering, Vol.85, pgs. 528-534.

Radaj, D., and Sonsino, C. M., 1998, "Fatigue Assessment of Welded Joints by Local Approaches", Abington Publishing, Abington, UK.

Ribeiro, A. S., 1993, "Efeito da fase de iniciação na previsão do comportamento à fadiga de juntas soldadas", PhD Thesis, University of Trás-os-Montes and Alto Douro, Vila Real, Portugal.

Taylor, N. et al, 2001, "Pressure Components Fatigue Design in the Framework of Directive 97/23/EC on Pressure Equipment", Final Report EC DG-ENTR, JRC-IAM.

Tricoteaux, A., Fardoun, F., Degallaix, S., Sauvage, F., 1995, "Fatigue Crack Initiation Life Prediction in High Strength Structural Steel Welded Joints", Fatigue and Fracture of Engineering Materials and Structures, Vol.18, No. 2, pp. 189-200.

Sanford, R. J., 1997, "Selected papers on foundations of linear elastic fracture mechanics", SEM Classic Papers, Volume CP1, Bethel, Connecticut, USA.

Walker, E. K., 1970, "The effect of the stress ratio during crack propagation and fatigue for 2024-T3 and 7075-T6 aluminium", Effects of environment and complex load history on fatigue life, ASTM-STP 462.

8. Responsibility notice

The authors are the only responsible for the printed material included in this paper.